Laser-wavelength dependence of mass-ablation rate and heat-flux inhibition in laser-produced plasmas

R. Fabbro, E. Fabre, F. Amiranoff, C. Garban-Labaune, J. Virmont, and M. Weinfeld
Groupe de Recherches Coordonnées I.L.M., Laboratoire de Physique des Milieux Ionisés, Ecole Polytechnique, 91128 Palaiseau Cédex, France

C. E. Max
Lawrence Livermore National Laboratory, Livermore, California 94550
(Received 14 July 1982)

Thin-foil experiments at 1.06, 0.53, and 0.26 μm have been realized in order to measure mass-ablation rate $\dot{m}$ as a function of absorbed laser flux ϕ_a and laser wavelength λ. The results can be put in the form $\dot{m}(\mathrm{kg/s\,cm^2}) \approx 110[\phi_a(\mathrm{W/cm^2})/10^{14}]^{1/3}\lambda_{\mu m}^{-4/3}$. Hydrodynamical simulations of these experiments show that heat-flux inhibition occurs at each wavelength, but the mechanisms are very different.

It has been shown that the great interest in using short-wavelength laser in laser fusion experiments results mainly from an increase of the absorption and a decrease of fast electron generation due to the dominance of collisional absorption.[1,2] Another interesting effect is also in the increase of the mass-ablation rate $\dot{m}$. We present in this Communication a measurement of $\dot{m}$ as a function of laser wavelength. The mass-ablation rate being directly related to the processes of heat transport in these plasmas,[3] we can therefore characterize such processes by numerical simulations of these experiments.

The experiments were carried out with a glass-neodymium laser rod; its output can be frequency doubled and quadrupled with potassium dihydrogen phosphate crystals with respective maximum efficiencies of 50 and 20% in energy. The corresponding pulse duration was monitored by a streak camera. The laser beam is focused onto the target by a 110-mm focal length quartz lens and the effective aperture of the focused beam is $f/1.2$.

Different methods were used in order to measure the intensity distribution in the focal spot: the diameters at half laser energy, which were 60, 50, and 70 μm at, respectively, 1.06, 0.53, and 0.26 μm, have been determined by analysis of impacts on burnpaper. These results agree with the measurement of light transmission through pinholes or with the diameter of x-ray pinholes photographs of the plasma. The targets used consist of thin polystyrene (CH) plane films whose thickness vary from 0.04 to 10 μm. The initial foil thickness being a parameter, we looked at different diagnostics which are sensitive to the amount of solid material which is heated during an experiment[4]: We measured the transmitted laser light through the foil by an $f/1$ rear lens whose aperture is larger than the focusing lens. If the transmission is different from zero, it means that all the foil has been heated in order to become underdense during the laser pulse; therefore we can determine the maximum foil thickness which can be heated during the laser pulse. We will define d_T, the foil thickness which gives 10% transmission. A second diagnostic concerns x-ray emission of the plasma. X-ray spectra were determined by a multichannel x-ray analyzer in the energy range between 1 and 60 keV. The x-ray emission for the 1–2-keV channel saturates above a characteristic foil thickness d_x; this means that no more material than d_x is heated during the laser pulse. Finally, with symmetric charge collectors, we looked at the symmetry of expansion of fast and thermal ions between the rear and the front side of the foil. The rear fast ion emission is directly related to the transport of fast electrons through the foil.[5] From thermal ions emission, the burnthrough depth is defined by determining the foil thickness d_i above which the time of flight of ions emitted at the rear side of the foil begins to be longer than the time of flight of the corresponding ions emitted at the front side. The interesting point is that, although these diagnostics are different, their corresponding characteristic burnthrough depths d_T, d_x, and d_i are very similar.[4] In fact, the hydrodynamic simulations of these diagnostics show that such a behavior is possible only when the heat flux is inhibited; in that case, these burnthrough depths can be directly used in order to measure the mass-ablation rate.

In Table I we give an example of the characteristic foil thickness d_T obtained experimentally by the transmission diagnostic for the three wavelengths used, as a function of the absorbed flux ϕ_A and the pulse width τ. The last column of Table I represents the value of A defined as $A = (\rho_0 d_T)/(\phi_a^{1/3}\lambda^{-4/3}\tau)$. One can see that, for our various experimental conditions, A is constant with value of 0.25 ± 0.04. If we define the mass-ablation rate $\dot{m}$ as $\dot{m} = (\rho_0 d_T)/\tau$, ρ_0

TABLE I. Experimental values of characteristic foil thickness d_T as a function of wavelength λ, absorbed flux ϕ_a, and pulse width τ. In the last column we have reported

$$A = \frac{\rho_0(\mathrm{g\,cm^{-3}})\, d_T(\text{Å})}{\phi_a^{1/3}(\mathrm{W\,cm^{-2}})\,\lambda_{\mu m}^{-4/3}\,\tau(\mathrm{ns})}.$$

λ (μm)	ϕ_{abs} (W/cm^2)	τ (ns)	d_T (μm)	A
	10^{14}	0.1	0.11	0.24
1.06	10^{15}	0.1	0.22	0.22
	1.5×10^{14}	2.5	3.7	0.28
	5×10^{14}	0.08	0.43	0.29
0.53				
	5×10^{13}	2	4.5	0.26
	1.3×10^{14}	0.06	0.45	0.25
0.26				
	2.7×10^{14}	0.17	1.5	0.23

being the solid density of the foil, and taking into account the definition of A, we obtain the experimental mass-ablation rate $\dot{m}$

$$\dot{m}\,(\mathrm{kg/s\,cm^2}) \approx 110\left(\frac{\phi_a(\mathrm{W/cm^2})}{10^{14}}\right)^{1/3}\lambda_{\mu m}^{-4/3}.$$

Recent results of experiments at 0.35 and 0.53 μm (Ref. 6) also agree with that formula. This scaling law can be obtained analytically when the mass-ablation rate is calculated in planar geometry and stationary ablative regime. This surprising agreement does not imply that our experimental conditions are stationary even if this model[7,8] shows that the conditions of realization of a stationary ablative regime can be satisfied more easily when one uses short-wavelength laser. Indeed, hydrosimulations give similar scaling law when the numerical description was obviously nonstationary; this point is clearly shown by curve (a) of Fig. 2.

The comparison of the picosecond experiments with planar hydrodynamical simulation allow us to determine the usual flux limit factor f. These simulations are performed with our 1D (one-dimensional) Lagrangian code FILM,[8] which uses a one-velocity, two-temperature formulation. Thermal heat flux is limited to the standard flux limit value defined by $0.6 f n_e v_e k T_e$. Suprathermal electron transport is described by a multigroup technique[9]; in contrast to the thermal electrons, they are classically treated without any flux limiter. Energy is absorbed by inverse bremsstrahlung and 20% of the energy reaching critical density is dumped into fast electrons with a hot-electron temperature T_H which is measured experimentally.[8]

An example of such a comparison is shown in Fig. 1, where it is plotted as a function of the flux limit

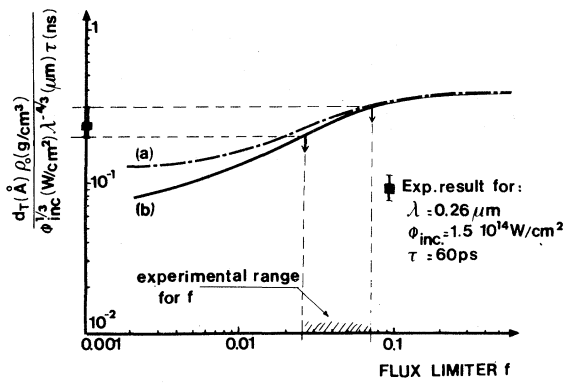

FIG. 1. Results of the simulations of the normalized values of d_T as a function of the flux limiter f for the experimental conditions given in the insert. We used inverse bremsstrahlung absorption and 20% of energy reaching critical density is dumped into fast electrons with $T_H = 1$ keV [curve (a)] or in thermal electrons [curve (b)]. ■ experimental value of A with corresponding error bars.

number f, the corresponding normalized value of d_T. In that case, for $\phi_{inc} = 1.5\times10^{14}$ W/cm^2, T_H was taken as 1 keV [curve (a)]. In order to check the efficiency of fast electron transport in this case, we dumped their energy into the thermal electrons at critical density [curve (b)]: the small difference of the two curves shows that, with these conditions, suprathermal transport is negligible. This can be expected due to the faster thermalization rate at this low hot-electron temperature. Experimentally, this point is confirmed by the observation of a negligible fraction of absorbed energy in fast ions. Consequently, taking into account the experimental uncertainties, the flux limiter f for the thermal population is such that $0.03 \lesssim f \lesssim 0.08$.

Similar analysis of the experiments at 1.06 μm is shown in Fig. 2; curve (a) corresponds to the case where all absorbed energy is dumped at critical density in thermal electrons. The agreement with experiments would imply a flux limit factor f of about 0.01. However, it is known that under these conditions at 1.06 μm, the main fraction of absorbed energy is given to the hot-electron component. This case is simulated by the curve (b) where 90% of absorbed energy is given in hot electrons and 10% in the thermal electrons; obviously, this does not agree with the experiments. The agreement can be observed with the curve (c) where 10% of absorbed energy is given to the hot electrons and 90% to the thermal electrons. This result means that only a maximum of 10% of the absorbed energy is used in a hot-electron longitudinal transport in the focal spot; the thermal transport being in all cases inhibited with f values ranging from 0.01 and 0.05, and depending on the fraction of energy given in the thermal electrons. Consequently, for our experimental conditions at

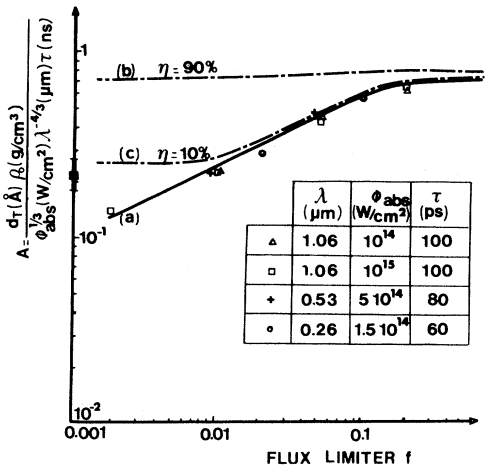

FIG. 2. Results of the simulations of the normalized value of d_T as a function of the flux limiter f; curve (a): for the conditions given in the insert the absorbed energy is dumped in thermal electrons at critical density. At 1.06 μm and $\phi_{abs}=10^{15}$ W/cm^2, curves (b) and (c) are for, respectively, 90 and 10% of absorbed energy going in fast electrons with $T_H=10$ keV. ■ corresponding experimental value of A (see Table I) with error bars.

1.06 μm, the absorbed energy being mainly transferred to the hot-electrons populations, this suggests that a significant fraction of these hot electrons do not contribute to the longitudinal transport but are lost in fast ion production and lateral transport.[10] The experiments on massive target at 1.06 μm with absorbed intensities of $\sim 10^{15}$ W/cm^2 are also consistent with that scheme; the important point is that one generally observes a large fraction ($\sim 30-50\%$) of absorbed energy in fast ions. This is only possible if the fast electrons are confined in the corona where they can make numerous bounces because, at each bounce, a fast electron loses only $\sim 3\%$ of its energy in fast ion acceleration.[11] Other diagnostics are also consistent with a reduction of the number of fast electrons which can enter in the solid target: experimental hard x-ray spectra obtained with massive targets[8] are much less intense that one could expect if all the fast electrons generated could freely enter into the solid. Magnetic fields of the order of 1 MG in the corona have been measured experimentally.[12] They could simply explain such nonclassical penetration of hot electrons into the target. A 10-keV electron in such a magnetic field has a radius of gyration of 3 μm, which is small compared to the scale length of the corona. In order to explain the observed fraction of energy in fast ions, some part of these hot electrons can be confined in these fields and lose a nonnegligible fraction of their energy; during this time they can also be deflected away from the focal spot and contribute to the lateral spreading of the energy.[13]

The experiments at 0.53 μm were analyzed in a similar way: compared to the 1.06-μm experiments, we observed a lower hot-electron temperature and a smaller fraction of absorbed energy in fast ions ($\lesssim 10\%$).[1,4] The experiments were reproduced with inverse bremsstrahlung absorption and 20% of the remaining energy reaching critical density being dumped into fast electrons, which are thermalized within the focal spot. For the thermal electrons, the flux limit number derived was such that $0.03 \lesssim f \lesssim 0.07$.[8]

In conclusion, heat-flux inhibition has been inferred in these experiments for the three wavelengths used. At 0.26 μm, fast electron transport is negligible and the thermal flux inhibition derived is roughly consistent with recent theoretical results[14] which show an important reduction of classical Spitzer conductivity. At 1.06 μm, fast electron generation dominates, and the experimental results are consistent with only a small fraction ($\sim 10\%$) of the absorbed energy being deposited on the foil at the focal spot. This effect can be considered as an effective inhibition of this population. Magnetic fields in the underdense corona could simply explain such a small coupling. They could lead to lateral spreading by 2D (two-dimensional) effects and also give rise to magnetic confinement of fast electrons in the corona. It is clear that these points need further investigation, more precisely by using 2D particle simulations in order to verify these fractions of lateral loss and fast particle generation.[13]

Another important result of these experiments concerns the scaling of the mass-ablation rate m^0 with the wavelength which shows a strong increase of m^0 at shorter wavelength. As a consequence, one can expect an increase of the ablation pressure and of the hydrodynamic efficiency. Additional experiments are undertaken in order to verify these points.

[1]GRECO I.L.M., Ecole Polytechnique Annual reports, 1978 and 1979 (unpublished); E. Fabre *et al.*, IAEA Report No. CN-38/1-4 (unpublished); A. Maaswinkel *et al.*, Phys. Rev. Lett. 42, 1625 (1979); D. C. Slater *et al.*, *ibid.* 46, 1199 (1981); W. Seka *et al.*, Opt. Commun. 40, 437 (1982); W. C. Mead *et al.*, Phys. Rev. Lett. 47, 1289 (1981).

[2]C. E. Max and K. G. Estabrook, Comments Plasma Phys. Controlled Fusion 5, 239 (1980).

[3]C. E. Max, C. F. McKee, and W. C. Mead, Phys. Fluids 23, 1620 (1980).

[4]F. Amiranoff, R. Fabbro, E. Fabre, C. Garban-Labaune, J. Virmont, and M. Weinfeld, Phys. Rev. Lett. 43, 522 (1979).

[5]G. D. Tsakiris, K. Eidman, R. Petsch, and R. Sigel, Phys. Rev. Lett. 46, 1202 (1981).
[6]J. D. Kilkenny *et al.*, Abstracts of the Eleventh Anomalous Absorption Conference, Montreal, June, 1981 (unpublished), Paper 4-4; B. Yaakobi *et al.*, Bull. Am. Phys. Soc. 26, 848 (1981).
[7]R. Fabbro, E. Fabre, and C. E. Max, Abstracts of the Eleventh Anomalous Absorption Conference, Montreal, June, 1981 (unpublished), Paper P-13.
[8]GRECO I.L.M., Ecole Polytechnique Annual Report, 1980 (unpublished).
[9]D. Shvaris, C. Jablon, I. B. Bernstein, J. Virmont, and P. Mora, Nucl. Fusion 19, 1457 (1979).
[10]N. A. Ebrahim *et al.*, Phys. Rev. Lett. 43, 1935 (1979); R. S. Martoribanks *et al.*, *ibid.* 45, 1798 (1980); D. M. Villeneuve *et al.*, *ibid.* 47, 515 (1981).
[11]P. Mora and R. Pellat, Phys. Fluids, 22, 2300 (1979).
[12]A. Raven *et al.*, Phys. Rev. Lett. 41, 554 (1978).
[13]D. W. Forslund and J. U. Brackbill, Bull. Am. Phys. Soc. 26, 873 (1981); R. Fabbro and P. Mora, Phys. Lett. 90A, 48 (1982).
[14]A. R. Bell, R. G. Evans, and D. J. Nicholas, Phys. Rev. Lett. 46, 243 (1981); D. Shvarts *et al.* (unpublished); R. J. Mason, Los Alamos Reports No. LA-UR-81-95 and No. LA-UR-81-390 (unpublished).